

*J. Nano- Electron. Phys.*  
3 (2011) No3, P. 5-14

© 2011 SumDU  
(Sumy State University)

PACS numbers: 73.61.Ga, 61.05.cp, 68.55.J, 88.37.Hk.

## PREPARATION AND PROPERTIES OF ZINC DOPED CADMIUM SELENIDE COMPOUNDS BY E-BEAM EVAPORATION

*N.J. Suthan Kissinger*<sup>1</sup>, *K. Perumal*<sup>2</sup>, *J. Suthagar*<sup>3</sup>

<sup>1</sup> Department of Physics, Jubail University College,  
Jubail Industrial City 31961, Saudi Arabia  
E-Mail: [suthanjkgmail.com](mailto:suthanjkgmail.com)

<sup>2</sup> Department of Physics, SRMV College of Arts & Science,  
Coimbatore-641020, India

<sup>3</sup> Department of Physics, Karunya University,  
Coimbatore-641114, India

*Cd<sub>1-x</sub>Zn<sub>x</sub>Se films with different zinc content were deposited by electron beam evaporation technique onto glass substrates for the application of solid-state photovoltaic devices. The structural, surface morphological and optical properties of Cd<sub>1-x</sub>Zn<sub>x</sub>Se films have been studied in the present work. The host material, Cd<sub>1-x</sub>Zn<sub>x</sub>Se, have been prepared by the physical vapor deposition method of electron beam evaporation technique (PVD: EBE) under a pressure of  $1 \times 10^{-5}$  mbar. The X-ray diffractogram indicates that these alloy films are polycrystalline in nature, hexagonal structure with strong preferential orientation of the crystallites along (002) direction. Linear variation of lattice constant with composition ( $x$ ) is observed. The optical properties shows that the band gap ( $E_g$ ) values varies from 2.08 to 2.64 eV as zinc content varies from 0.2 to 0.8. The surface morphological studies show the very small, fine and hardly distinguishable grains smeared all over the surface. It is observed that the grain size is decreasing with increasing zinc content.*

**Keywords:** CADMIUM SELENIDE, ZINC SELENIDE, ELECTRON BEAM, EVAPORATION, OPTICAL PROPERTIES.

(Received 12 June 2011, in final form 07 July 2011  
published online 05 November 2011)

### 1. INTRODUCTION

The interest in Cd<sub>1-x</sub>Zn<sub>x</sub>Se ternary systems are increasing rapidly during the present decade, because the lattice constants and band gap values can be tuned systematically by incorporating various atomic constant of Zn( $x$ ). Such variations facilitate the development of new optoelectronic and electronic devices. These alloy systems are attractive semiconductor materials for light emitting devices in different colors (blue to red spectral region) [1].

The band gap of this material can be tuned from 1.70 to 2.70 eV with  $0 \leq x \leq 1$ . It is an efficient absorber in the visible region of solar spectrum [2]. The applications of Cd<sub>1-x</sub>Zn<sub>x</sub>Se in thin film devices like laser screen materials in projection color TV's [3], nuclear radiation detectors, light emitting diodes, laser diodes, electroluminescent, photoluminescent, photovoltaics [4], etc. have shown its prominence and ability. The band structures, optical

properties and crystal structures of both CdSe and ZnSe are very similar and therefore the system  $\text{Cd}_{1-x}\text{Zn}_x\text{Se}$  would not only result in the feasibility of graded energy gap of a broad spectral sensitivity but many more material characteristics can be altered and excellently controlled by the system composition  $x$ . Both CdSe and ZnSe are known to exist in either cubic zinc blende or hexagonal wurtzite crystal forms depending on the composition and the conditions of preparation. Compared to CdSe,  $\text{Cd}_{1-x}\text{Zn}_x\text{Se}$  is more stable and would replace CdS as a window material in solar cells. Further, the incorporation of ZnSe into CdSe has shown pronounced effect in enhancing the electrochemical power conversion efficiency [5-7].

The use of thin film polycrystalline semiconductors has attracted much interest in an expanding variety of applications in various electronic and optoelectronic devices. The technological interest in polycrystalline-based devices is mainly caused by their very low production costs. Different researchers [8-10] prepared  $\text{Cd}_{1-x}\text{Zn}_x\text{Se}$  films by different techniques and studied their structural, optical and photoelectrochemical properties. In the present study we have prepared  $\text{Cd}_{1-x}\text{Zn}_x\text{Se}$  films by electron beam evaporation technique at  $100^\circ\text{C}$  with various zinc content incorporated with cadmium as  $x = 0.2, 0.4, 0.6$  and  $0.8$  and their structural, optical and surface morphological properties were studied. All the films of  $\text{Cd}_{1-x}\text{Zn}_x\text{Se}$  system were deposited under the same experimental conditions.

## 2. EXPERIMENTAL DETAILS

Thin films of  $\text{Cd}_{1-x}\text{Zn}_x\text{Se}$  with different Zn composition were deposited from CdSe and ZnSe powder (Aldrich, 99.99 %) by electron beam evaporation technique using a HINDHIVAC Vacuum coating unit (model: 12A4D) fitted with electron beam power supply (model: EBG-PS-3K). For the EB evaporation of  $\text{Cd}_{1-x}\text{Zn}_x\text{Se}$  solid solutions, CdSe and ZnSe binary compounds are mixing in various atomic proportion and used as the precursor powder pellet for depositing the film. If the CdSe and ZnSe powder samples were heated using an electron beam collimated from the d.c heated tungsten filament cathode, the sample particles were spread out of the graphite crucible. For the betterment of homogeneous and uniform deposition on the substrate surface, the  $\text{Cd}_{1-x}\text{Zn}_x\text{Se}$  pelletized targets have been utilized. Before making the pellets, the powder mixtures were ground in an agate mortar for 3 hours to get uniformly mixed powders. Pellets were made at a pressure of  $10 \text{ tons/cm}^2$  and heated at  $100^\circ\text{C}$  for one hour. Since  $\text{Cd}_{1-x}\text{Zn}_x\text{Se}$  films with  $x = 0, 0.2, 0.4, 0.6, 0.8$  and  $1.0$  were planned to be deposited on glass substrates and taking into consideration the different melting points of CdSe and ZnSe and vapor pressure of Cd, Zn and Se elements. The different preparation parameters such as, source to substrate distance (12 cm) and partial pressure ( $10^{-5}$  mbar) have been varied and optimized for depositing uniform, well adherent and transparent films. The films were found to be uniform, porous free and adhered well with the glass plates.

The crystalline size ( $D$ ) was calculated from the full width at half maximum (FWHM) ( $\beta$ ) by using the Scherrer formula:

$$D = 0.94\lambda/(\beta\cos\theta) \quad (1)$$

where  $\lambda$  is the wavelength of the X-ray used, and  $\theta$  is half the angle between the incident and the scattered X-ray beams.

The lattice spacing ( $d$ ) is calculated from the Bragg's formula

$$d = 0.5\lambda/\sin\theta. \quad (2)$$

The lattice parameter ( $a$ ) is determined for the cubic structure by using the following expression:

$$1/d^2 = (h^2 + k^2 + l^2)/a^2, \quad (3)$$

where  $h, k, l$  are the Miller indices of the lattice plane.

The spectral normal transmittance ( $T$ ) was measured by UV-vis-nir spectrophotometer over the wavelength range 300-2500 nm. The calculation of absorption coefficient  $\alpha$  gives a higher value of  $10^4 \text{ cm}^{-1}$  near the absorption edge and in the visible region.  $\alpha$  depends on the radiation energy and on the composition of the films. The absorption data were analyzed using the relation for the near edge absorption of direct bandgap semiconductor films

$$\alpha = K(h\nu - E_g)^{0.5}/h\nu. \quad (4)$$

The structural properties of the films were studied by the JEOL JDX X-ray diffractometer (XRD) using  $\text{CuK}_\alpha$  radiation ( $\lambda = 1.5418 \text{ \AA}$ ) with Ni filter. The optical spectra were recorded in the wavelength range 300-2500nm using UV-Vis-NIR spectrophotometer (Hitachi V-3400). Surface morphology of the films was studied by JEOL JSM-5610 L V (Japan) scanning electron microscope (SEM).

### 3. RESULTS AND DISCUSSION

The XRD patterns of the EB evaporated  $\text{Cd}_{1-x}\text{Zn}_x\text{Se}$  thin films were recorded to study the nature, phase and structure with different zinc ( $x$ ) content introduced into the CdSe matrix. Figure 1a-d shows the XRD spectra of  $\text{Cd}_{1-x}\text{Zn}_x\text{Se}$  films with  $x = 0.8, 0.6, 0.4, 0.2$ .

The sharp and well defined peaks indicate the polycrystalline nature of fabricated films. A high intense peak observed at  $2\theta = 25.62^\circ$  corresponding to (002) reflection and another peak very close to it at  $2\theta = 24.18^\circ$  is assigned to (100) reflection with a reduced intensity. The strong peak at  $25.62^\circ$  confirms the presence of hexagonal structure for all the films with highly textured orientation along (002) plane. Further,  $2\theta$  values are found to shifted towards higher angle side with increasing zinc content. This is a confirmative evidence of formation of homogeneous and alloyed  $\text{Cd}_{1-x}\text{Zn}_x\text{Se}$  films by EB evaporation technique. Further, the presence of (002) preferred orientation indicates that the crystallites are oriented with their c-axis perpendicular to the substrate. The lattice space  $d$  values agree well with the reported XRD data [11] for the  $\text{Cd}_{1-x}\text{Zn}_x\text{Se}$  films deposited by electrochemical technique. Table 1 gives the lattice parameter values derived from XRD spectra for the  $\text{Cd}_{0.8}\text{Zn}_{0.2}\text{Se}$ ,  $\text{Cd}_{0.6}\text{Zn}_{0.4}\text{Se}$ ,  $\text{Cd}_{0.4}\text{Zn}_{0.6}\text{Se}$  and  $\text{Cd}_{0.2}\text{Zn}_{0.8}\text{Se}$  thin films.

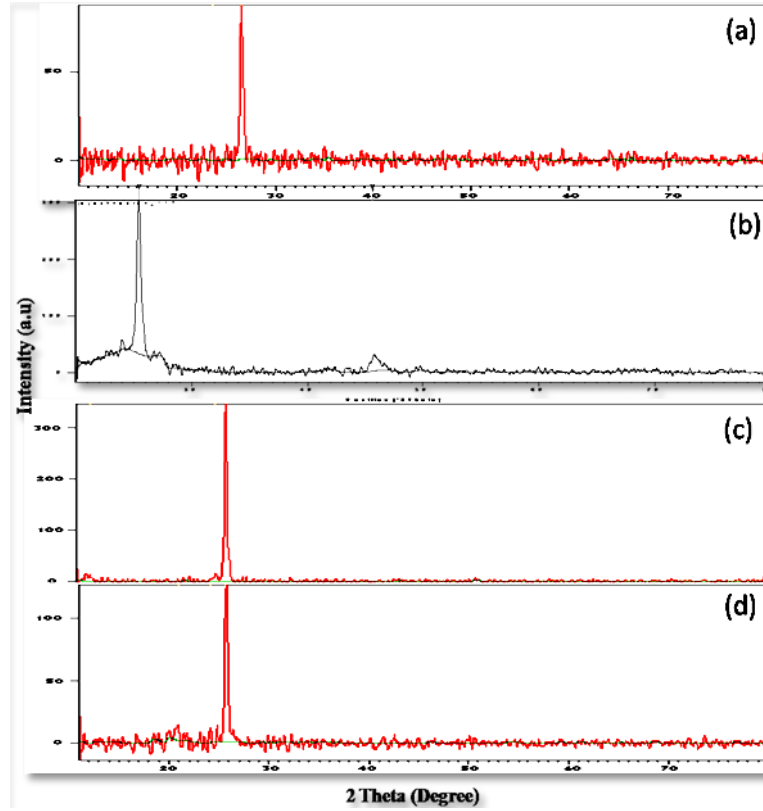


**Fig. 1** – XRD spectrum obtained for  $\text{Cd}_{1-x}\text{Zn}_x\text{Se}$  films with different  $x$  content  
(a)  $x = 0.2$  (b)  $x = 0.4$ , (c)  $x = 0.6$ , (d)  $x = 0.8$

**Table 1** – Lattice parameter values derived from XRD spectra for the  $\text{Cd}_{0.8}\text{Zn}_{0.2}\text{Se}$ ,  $\text{Cd}_{0.6}\text{Zn}_{0.4}\text{Se}$ ,  $\text{Cd}_{0.4}\text{Zn}_{0.6}\text{Se}$  and  $\text{Cd}_{0.2}\text{Zn}_{0.8}\text{Se}$  thin films

$\text{Cd}_{1-x}\text{Zn}_x\text{Se}$ Film	(h k l)	$2\theta$ (Deg)	$D$ (nm) Experimental	$c$ (nm)	$a$ (nm)	$c/a$ (nm)
$\text{Cd}_{0.8}\text{Zn}_{0.2}\text{Se}$	(1 0 0)	24.17	0.3682	0.693	0.425	1.631
	(0 0 2)	25.69	0.347(1 1 1)	-	-	-
$\text{Cd}_{0.6}\text{Zn}_{0.4}\text{Se}$	(1 0 0)	24.87	0.358	0.682	0.413	1.651
	(2 0 0)	26.51	0.337(1 1 1)	-	-	-
$\text{Cd}_{0.4}\text{Zn}_{0.6}\text{Se}$	(1 0 0)	26.59	0.335	0.671	0.392	1.711
	(2 0 0)	28.33	0.319(1 1 1)	-	-	-
$\text{Cd}_{0.2}\text{Zn}_{0.8}\text{Se}$	(1 0 0)	26.95	0.331	0.658	0.384	1.713
	(2 0 0)	28.49	0.311(1 1 1)	-	-	-

The variation in lattice parameter with different Zn concentration is shown in Figure 2a-c. The lattice parameter values  $c$  and  $a$  were calculated on assuming hexagonal structure for all  $\text{Cd}_{1-x}\text{Zn}_x\text{Se}$  films, given in Table 1. The value of  $c$  decreased from 0.693 to 0.658 nm while that of  $a$  decreased from 0.425 to 0.384 nm with increasing Zn content confirming the solid solution formation between CdSe and ZnSe binary compounds to make

various ternary alloys. Further, the lattice parameters of these films follow the Vegard's law which means that the lattice parameters of  $\text{Cd}_{1-x}\text{Zn}_x\text{Se}$  ternary alloys, with Zinc content  $x$  can be linearly varies from the lead binary alloy CdSe. The slight variation in  $c/a$  ratio was observed when the zinc concentration was increased from 0.2 to 0.8. When the zinc concentration was increased from 0.2 to 0.8, the  $c/a$  ratio was increased from 1.63 to 1.73. Husain et al [12] have reported the cubic structure for the whole range of Zinc content from  $x = 0.2$  to 0.8 for their sintered films. This result predicts that these ternary alloys have hexagonal structure and that CdSe-ZnSe system forms excellent solid solutions in mixing by the exact substitution of Zn in the atomic locations of Cd.

The optical transparency of CdZnSe films for different Zn concentrations recorded at room temperature for 300-2500 nm wavelength range is shown in Figure 3. The average transmission in the visible range slightly decreases (from 80 % to 65 %) as the Zn concentration in the starting material increases. Figure 4 shows the optical energy band gap spectrum of EB evaporated  $\text{Cd}_{1-x}\text{Zn}_x\text{Se}$  films. The optical band gap values were obtained by extrapolating the linear portion of the  $(\alpha h\nu)^2$  vs  $h\nu$  plot. The  $E_g$  values for our films vary from 2.08 to 2.64 eV as zinc content varies from 0.2 to 0.8. An increase in band gap is attributed to the mixing of higher band gap material, ZnSe with smaller band gap material CdSe. The variation of  $E_g$  is sub-linear with zinc incorporation into the CdSe lattice. All the films are observed to have direct band gap transition, as that of the end components

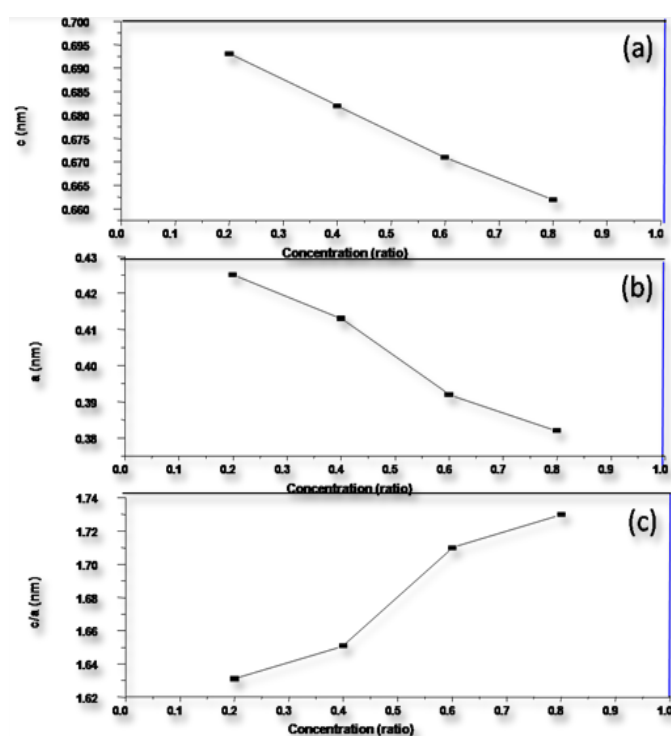


**Fig. 2** – Variation of lattice parameter (a)  $c$  value with concentration (b)  $a$  value with concentration, (c)  $c/a$  value with concentration

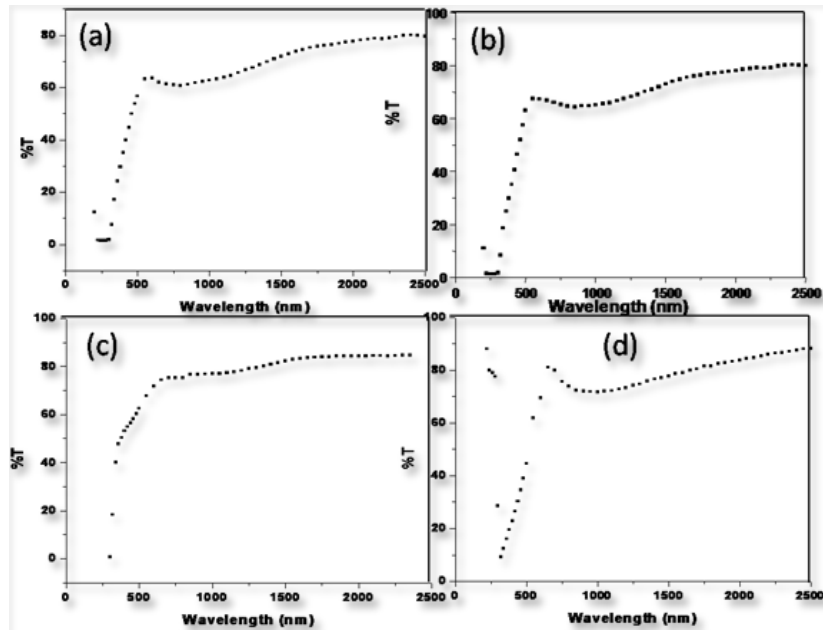


**Fig. 3** – Transmission spectra of  $\text{Cd}_{1-x}\text{Zn}_x\text{Se}$  films with  $x = 0.2$  (a),  $x = 0.4$  (b),  $x = 0.6$  (c),  $x = 0.8$  (d)

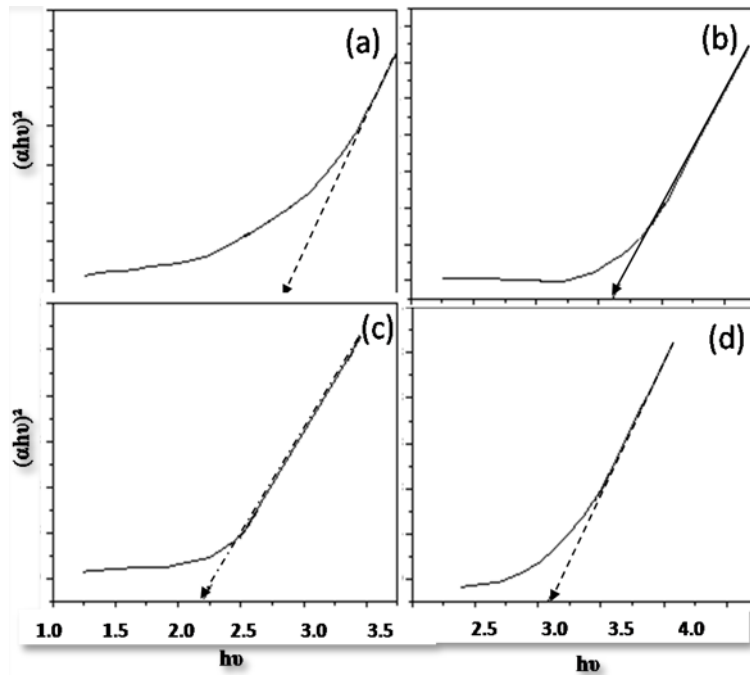


**Fig. 4** –  $(\alpha h\nu)^2$  vs  $h\nu$  plot for the  $\text{Cd}_{1-x}\text{Zn}_x\text{Se}$  films with  $x = 0.2$  (a),  $x = 0.4$  (b),  $x = 0.6$  (c),  $x = 0.8$  (d)

behave. The continuous variation of  $E_g$  with  $x$  confirms the solid solution formation between CdSe and ZnSe so that their optical and electronic properties can be tailored. The variation of  $E_g(x)$  with increasing zinc content shows a sub-linear behavior, shows a lowering phenomenon in the alloy films of  $\text{Cd}_{1-x}\text{Zn}_x\text{Se}$ . The bandgap values of the end materials (CdSe & ZnSe) in our present series of study are 1.92 and 2.95 eV respectively.

The SEM pictures of  $\text{Cd}_{1-x}\text{Zn}_x\text{Se}$  films on glass substrates are shown in Figure 4. SEM is a promising technique for the topography study of samples, as it provides valuable information regarding the growth mechanism, shape and size of the particles and/or grains. The image of the deposited film reveals the uniform surface nature. Surface morphology by SEM studies shows very small, fine and hardly distinguishable grains smeared all over the surface. This is the characteristic features of zinc rich surfaces. It is clearly observed from the surface morphological studies by scanning electron microscope that all the films have surfaces with uniform, homogeneous grain morphology. No crack was observed on the surface of the films. The sharp cleavage edge indicates the well adhesive nature of the films onto the substrates.

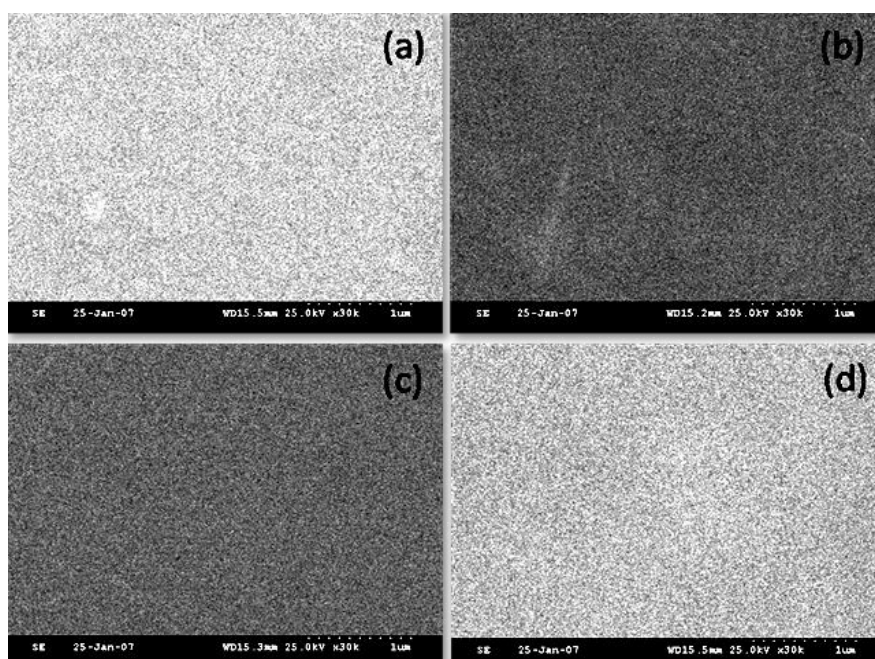


**Fig. 5** – SEM pictures taken for  $\text{Cd}_{1-x}\text{Zn}_x\text{Se}$  films with  $x = 0.2$  (a),  $x = 0.4$  (b),  $x = 0.6$  (c),  $x = 0.8$  (d)

To visualize the film surface, two dimensional (2D) AFM pictures are given in Figure 6 a-d for the  $\text{Cd}_{1-x}\text{Zn}_x\text{Se}$  films with zinc contents  $x = 0.2, 0.4, 0.6$  and  $0.8$  respectively. It can be easily observed that the grain size is decreasing with increasing zinc content. This is acceptable because the atomic radius of Zn is 0.138 nm which is less than the atomic radius of Cd 0.171 nm. The presently studied  $\text{Cd}_{1-x}\text{Zn}_x\text{Se}$  film makes very good solid solution which means that zinc atoms replace cadmium atoms in the crystal lattice. This will obviously reduce

the dimension of the lattice leading to the formation of linear grains with reduced grain size when one mixes to CdSe various amount of ZnSe. For comparison, 2D AFM pictures are also given in Fig.6 e and f respectively for CdSe and ZnSe films. The calculation of average surface roughness ( $R_a$ ) values for these films show very low values 0.12, 0.13, 0.20 and 0.16 nm respectively. Such very low values predict the uniform surface of the  $Cd_{1-x}Zn_xSe$  film prepared by the EB evaporation technique in the present study. It shows the compactness, pinhole free and well adherent nature of these films on glass substrates which will be very much useful for PEC devices. The line profile curves given under each 2D AFM pictures confirm our discussions.

Figure 7a-d shows the PL spectra recorded at room temperature for various Zn contents 0.2, 0.4, 0.6 and 0.8 respectively. The PL spectrum shifts towards higher energy values with increasing zinc content  $x$ , due to the increase of fundamental gap with ZnSe composition. Each PL spectrum is characterized by its Near Band Edge (NBE) recombination as suggested for the  $CdS_xSe_{1-x}$  films prepared by pulsed laser deposition technique [13]. There is no PL report on the full range of solid solutions with zinc content

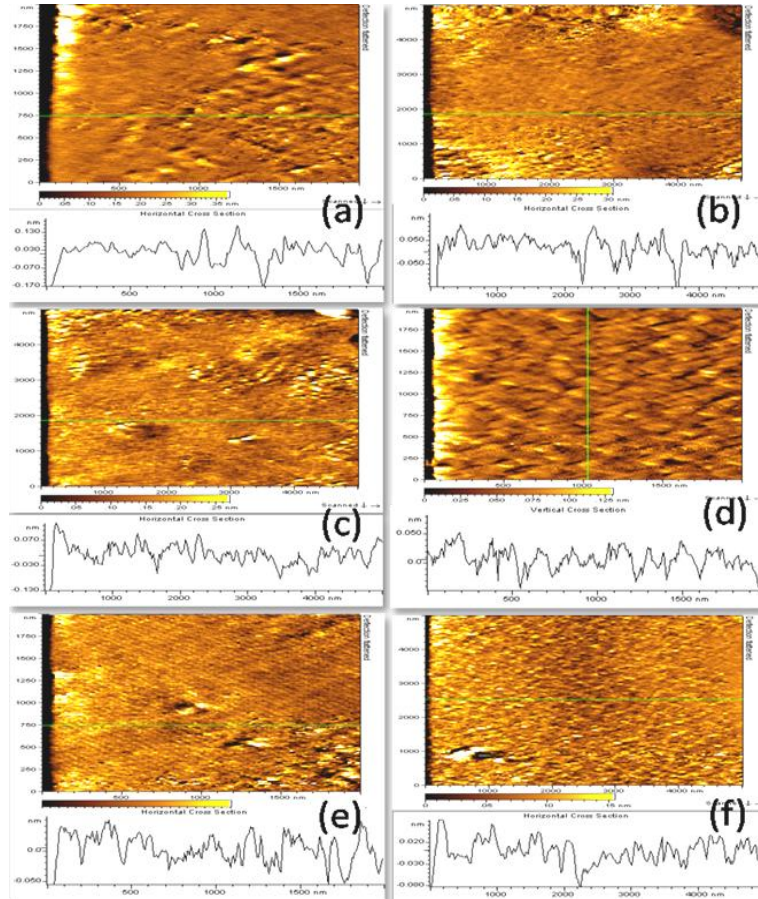


**Fig. 6** – AFM pictures (2D) taken for the  $Cd_{1-x}Zn_xSe$  films with (a)  $Cd_{0.2}Zn_{0.8}Se$  (b)  $Cd_{0.4}Zn_{0.6}Se$  (c)  $Cd_{0.6}Zn_{0.4}Se$  (d)  $Cd_{0.8}Zn_{0.2}Se$  (e) CdSe (f) ZnSe



$x = 0$  to 1.0. Toropov et al. [14] have the PL excitonic spectrum in super lattices (SLs) of CdSe insertions in a ZnSe matrix for elucidating the CdSe/ZnSe interface morphology. They have obtained a PL peak at 5 K for Cd<sub>0.23</sub>Zn<sub>0.77</sub>Se single Quantum Well (QW) at about 2.77 eV with 0.4 ML (monolayer) and at 2.73 eV with 1.15 ML. For our film with composition Cd<sub>0.2</sub>Zn<sub>0.8</sub>Se, the peak is observed at about 2.65 eV which is lower compared to ML films. It is natural that our films have thickness in the 200 nm where as ML layers of thickness are in the range about 4 to 12 nm and the effect of nano dimensional cones into play. Similarly PL studies for multiply stacked CdSe quantum-dot (QD) arrays with a large ZnSe space thickness were conducted by Kirm et al. [15]. Their PL spectrum at 20 K showed a broad peak at 2.45 eV, this value is found to be near to the PL peak at 2.41 eV observed in the present work for the films Cd<sub>0.6</sub>Zn<sub>0.4</sub>Se. The bandgap and PL peak intensity values of Cd<sub>1-x</sub>Zn<sub>x</sub>Se films for different zinc content is given in Table 2. Comparison of these results confirm that the Cd<sub>1-x</sub>Zn<sub>x</sub>Se solid solution films deposited by EB evaporation technique in this study are of device quality nature and can be used for PEC solar cells and light emitting diode studies.

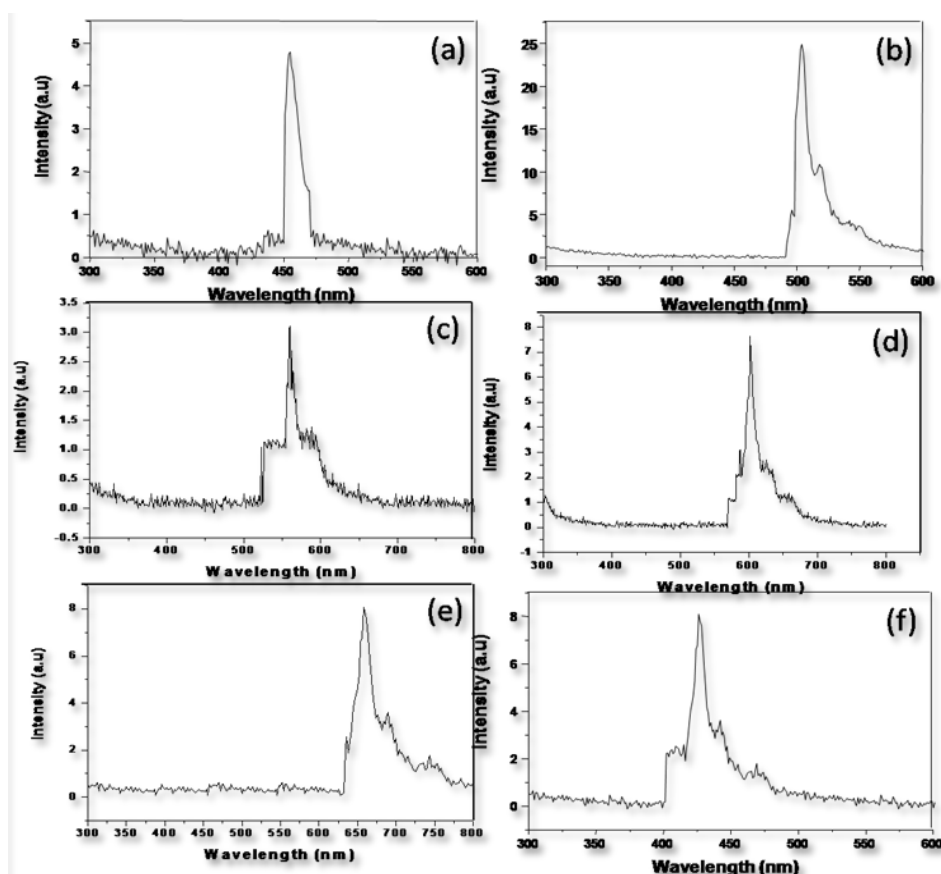


**Fig. 7** – PL spectrum obtained for the Cd<sub>1-x</sub>Zn<sub>x</sub>Se films with  $x = 0.2$  (a),  $x = 0.4$  (b),  $x = 0.6$  (c),  $x = 0.8$  (d), CdSe (e), ZnSe (f)

**Table 2** – The bandgap ( $E_g$ ) and PL peak intensity for different zinc content

Film Composition	Bandgap Value ( $E_g$ ) eV	PL Peak Intensity (nm)
CdSe	1.92	440
Cd <sub>0.8</sub> Zn <sub>0.2</sub> Se	2.08	455
Cd <sub>0.6</sub> Zn <sub>0.4</sub> Se	2.20	510
Cd <sub>0.4</sub> Zn <sub>0.6</sub> Se	2.42	560
Cd <sub>0.2</sub> Zn <sub>0.8</sub> Se	2.64	605
ZnSe	2.95	655

#### 4. CONCLUSIONS

Ternary chalcogenide alloys of CdSe and ZnSe have been prepared by electron beam evaporation technique. In this paper we have described the detail study of the structural, optical and surface morphological properties of Cd<sub>1-x</sub>Zn<sub>x</sub>Se films prepared by electron beam evaporation technique. The X-ray diffraction analysis clearly shows the formation of predominant peaks along (0 0 2) growth orientation which exhibits that these alloy films are polycrystalline nature and hexagonal structure. The better aligned and highly oriented growth peaks enumerate the stoichiometric nature of the films. The XRD result predicts that these ternary alloys all have hexagonal structure and that CdSe-ZnSe system forms excellent solid solutions in all mixings by the exact substitution of Zn in the atomic locations of Cd. The optical analysis reveals that the variation of  $E_g(x)$  with increasing zinc content shows a sub-linear behavior, shows a lowering phenomenon in the alloy films of Cd<sub>1-x</sub>Zn<sub>x</sub>Se. The nano structural nature of Cd<sub>1-x</sub>Zn<sub>x</sub>Se films is evident from the surface morphological results. We believe that these preliminary characteristic observations on the EB evaporated Cd<sub>1-x</sub>Zn<sub>x</sub>Se films will be helpful to explore the device performance of the films.

#### REFERENCES

1. M. Husain, B.P. Singh, S. Kumar, T.P. Sharma, P.J. Sebastian, *Sol. Energ. Mat. Sol. C* **76**, 399 (2003).
2. M. Kumar, M.K. Sharan, M. Sharon, *Sol. Energ. Mat. Sol. C* **51**, 35 (1998).
3. K.C. Sharma, J.C. Garg, *Indian J. Pure Ap. Phy.* **26**, 480 (1998).
4. N.J. Suthan Kissinger, M. Jayachandran, K. Perumal, C. Sanjeeviraja, *Bull. Mater. Sci.* **30**, 547 (2007).
5. G. Perna, V. Capozzi, M. Ambrico, V. Augelli, T. Ligonzo, A. Minafra, L. Schiavulli, M. Pallara, *Appl. Surf. Sci.* **233**, 366 (2004).
6. B. Tippelt, J. Breitschneider, P. Hahner, *phys. status solidi A* **163**, 11 (1997).
7. C. Natrajan, G. Nogami, M. Sharon, *Bull. Electrochem.* **12**, 136 (1996).
8. K.Y. Rajpure, S.M. Bamane, C.D. Lokhande, C.H. Bhonsale, *Indian J. Pure Ap. Phy.* **37**, 413 (1999).
9. U. Lunz, J. Kuhn, F. Goschenhofer, S. Einfeldt, C.R. Becker, G. Landwehr, *J. Appl. Phys.* **80**, 6861 (1996).
10. K.B. Kale, C.D. Lokhande, *Appl. Surf. Sci.* **253**, 3109 (2007).
11. R. Chandramohan, T. Mahalingam, J.P. Chu, P.J. Sebastian, *Sol. Energ. Mat. Sol. C* **81**, 371 (2004).
12. R.B. Kale, C.D. Lokhande, *Appl. Surf. Sci.* **223**, 343 (2004).
13. G. Perna, S. Pagliara, V. Capoyzi, M. Ambrico, T. Ligonzo, *Thin Solid Films* **349**, 220 (1999).
14. A. Toropov, T.V. Shubina, S.V. Socokin, R.N. Kyutt, S. V. Ivanov, G. R. Pozina, J.P. Bergman, B. Monemar, M. Karlsteen, *Appl. Surf. Sci.* **166**, 278 (2000).
15. T.W. Kim, D.C. Choo, D.C. Lee, M. Jung, J.W. Cho, K.H. Yoo, S. Lee, K.Y. Seo, J.K. Furdyna, *Solid State Commun.* **122**, 229 (2002).